

LOCAL DEFORMATION BEHAVIOUR OF HIGH-STRENGTH PM-TOOL STEELS

Peter J. Gruber^{a, b}, Gerhard Jesner^b, Reinhold Ebner^a, Otmar Kolednik^c

^a Materials Center Leoben Forschung GmbH, Roseggerstrasse 12, 8700 Leoben, Austria

^b Böhler Edelstahl GmbH & CoKG, Mariazellerstrasse 25, 8605 Kapfenberg, Austria

^c Erich Schmid Institute of Materials Science, Austrian Academy of Sciences,
Jahnstrasse 12, 8700 Leoben, Austria

Keywords

Tool steel, powder metallurgy (PM), high strength tool steels, cutting edge, local deformation behaviour, digital image analysis,

Abstract

The paper examines the local deformation behaviour of a powder metallurgically produced (PM) tool steel, that is used for stamping and cutting dies. The local deformation behaviour was investigated using an in-situ compression test. In order to observe the local deformation behaviour of the tool steels, images are taken in the scanning electron microscope at several loading steps. Using digital image analysis, the local strain and rotation fields of the deformed regions were evaluated. Up to now this methodology has been applied only for materials with low yield strengths. Furthermore, a more practise-relevant testing procedure with special cyclic loading equipment and new split specimens is developed, in order to study the local plastic strains in high-strength tools near a cutting edge.

^a Corresponding author, Tel.: +43 3842 804 314; fax: +43 3842 804 116
E-mail address: peter.gruber@mcl.at

1. Introduction

The greater demand for lightweight structures causes a trend towards the development and increased use of high strength steel grades for structural applications, especially in the automotive industry. Higher strength of the work-piece material requires higher strength tool steels. Therefore tool steels with an improved performance to withstand the large loads for stamping, cutting and blanking of high strength structural steels will be required in future [1,2]. The increased strength of the work-piece materials causes an increase in the loading of the tools used for stamping and cutting. The higher tool loading is often responsible for increased tool wear and unexpected catastrophic tool failure at low number of cycles.

A large variety of different steels, ranging from low alloyed steels up to high speed steels, are used for manufacturing tools such as shears, punches and blanking dies [3]. Highest performance for stamping, cutting and blanking tools is mainly achieved with high performance powder metallurgy (PM) tool steel grades [4]. The loading conditions of the edges of stamping, cutting and blanking tools are very complex. The material at the work-piece flows around the edge of the tool and causes high normal and shear stresses. These high stresses lead to a high risk for plastic deformation or micro-chipping of the tool edge. Previous studies revealed that a build-up of tensile residual stress occurs near the edge [5, 6]. Recent investigations have shown that plastic deformation takes place even at distances up to several tenths of a millimetre from the cutting edge and high plastic deformations can occur directly at the edge or near the tool surface [7]. Since the tool is cyclically loaded during service its life time is strongly affected by local plastic deformation. Therefore, it is important to study the local deformation behaviour of these high strength materials. The aim of this paper is to introduce procedures for the investigation of the local deformation behaviour of such high strength steels under monotonic and cyclic loading conditions.

2. Material

A PM-tool steel with the designation Böhler S390 Microclean was investigated. The chemical composition is shown in Table 1. The rough machined specimens were austenitized in vacuum and subsequently quenched in liquid nitrogen. Then the specimens were annealed to a target hardness of 62HRC. The microstructure of the heat treated material consists mainly of primary carbides embedded in a tempered martensite matrix. Figure 1 shows a scanning electron microscope (SEM) micrograph of the microstructure. Two types of primary carbides are visible, white M_6C and grey MC carbides, both have an average size of $1\mu m$. The volume fraction of the primary carbides is about 20%. The data of the steel from a tensile test is shown in Table 2. Given are the Rockwell hardness, the yield strengths at 0.1% ($R_{p0.1}$) and 0.2% ($R_{p0.2}$) strain, the tensile strength (R_m), the uniform strain (A_g) and the elongation at fracture (A).

Table 1: Chemical composition of the PM-tool steel in weight percent

| Steel grade | C % | Cr % | W % | Mo % | V % | Co % |
|------------------------|------|------|------|------|-----|------|
| Böhler S390 Microclean | 1.64 | 4.8 | 10.4 | 2.0 | 4.8 | 8.0 |

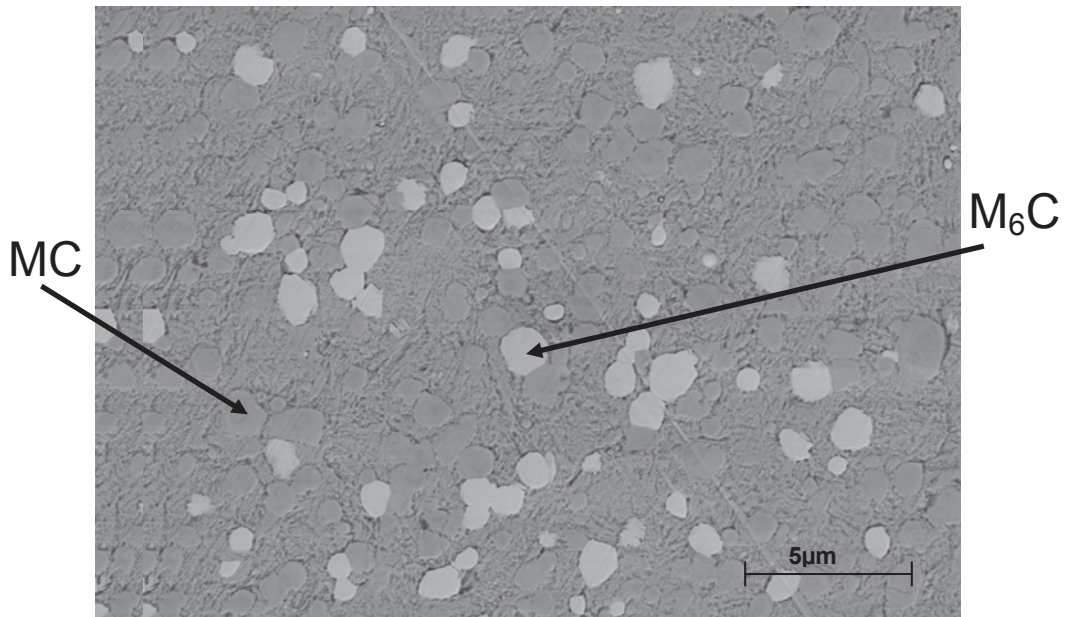


Figure 1: SEM micrograph of the PM-tool steel grade Böhler S390 Microclean

Table 2: Mechanical properties of the PM-tool steel

| Steel grade | hardness | $R_{p0.1}$ | $R_{p0.2}$ | R_m | Ag | A |
|------------------------|----------|------------|------------|-------|------|------|
| | [HRC] | [MPa] | [MPa] | [MPa] | [%] | [%] |
| Böhler S390 Microclean | 62,30 | 2270 | 2460 | 2810 | 1,51 | 1,84 |

3. Deformation behaviour under monotonic loading

3.1. Experimental

In order to study the local deformation behaviour of materials with very high yield stress it is necessary to apply an in-situ compression test instead of the conventional in-situ tensile test that have been used for low-strength materials [8, 9]. The compression specimens have a cross section of $1.4 \times 1.4 \text{ mm}^2$ and a length of 2.15 mm. Reasons for these dimensions are the capacity of the load cell (10000N) of the self built compression equipment and the ratio between height and width of the specimens that should be 1.5 [11]. The samples were carefully ground and mechanically polished with different diamond suspensions. A heat treatment in a vacuum oven was performed to relieve residual stresses in the specimens. To get better information about the microstructure, samples were etched slightly with a 10% HNO_3 acid. After the preparation, each specimen was loaded in discrete steps in compression equipment. Images with a resolution of 2048×1536 pixels were taken in the SEM from the unloaded specimen and after different stages of deformation (every $100 \mu\text{m}$). In Figure 2 a schematic picture of the in-situ compression testing procedure is shown.

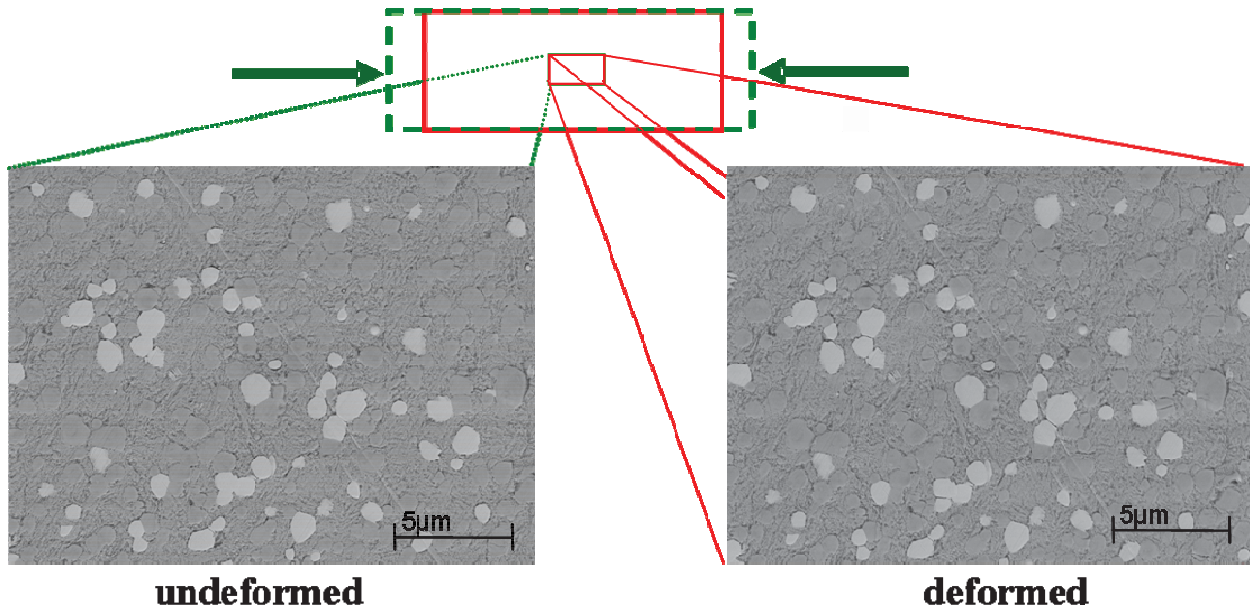


Figure 2: Schematic picture of the in-situ compression testing procedure.

To analyse the in-situ test, an automatic local deformation procedure was used [8, 12]. The procedure, called “matching”, is based on the automatic detection of identical points in two micrographs that are taken at different stages of deformation. These corresponding points, called “homologue points”, can be detected with an accuracy of approximately 0.05 pixels [8]. The density of homologue points lies between 3 and 6 points per 100 pixels. This means that 380,000 to 740,000 homologue points are found in each pair of deformation micrographs [9]. From the displacement vector of the homologue points the in-plane strain and rotation fields are derived by numerical differentiation [8]. For each load step, maps of local strain distribution were generated. Maps of the tensile strains in loading direction, ε_{xx} , the transverse strains, ε_{yy} , the shear strains, ε_{xy} and the rotation, r_{xy} were rendered. The analysis of the deformation micrographs is described in more detail in [8]. In [9, 10] the procedure has been applied to aluminum based metal matrix composites.

3.2. Results and discussion

To demonstrate the results of the compression test, only two examples of maps with normalized strain in compression direction are described. The size of the analyzed region is about $15 \times 20 \mu\text{m}$. The loading direction is parallel to the horizontal axis (x) of the pictures. The results of the compression test are summarised in Figure 3 and Figure 4. Figure 3a shows the microstructure of the sample at a global deformation stage of $\varepsilon_{\text{global}} \approx 2\%$ and Figure 3b shows the microstructure at $\varepsilon_{\text{global}} \approx 8\%$. The micrographs of the microstructure do not exhibit areas of visible damage (e.g. cracked carbides or carbide/matrix interfaces). Note that the elongation at fracture in tension is $A = 1.84\%$. Figure 4 presents the maps of the normalised strain in loading direction κ_{xx} at two different stages of deformation, $\varepsilon_{\text{global}} \approx 2\%$ and 8% . The normalised strains are the local strains related to the global strain $\kappa_{xx} = \varepsilon_{xx} / \varepsilon_{\text{global}}$. Normalised strains are used to simplify the comparison of the different deformation stages. The x - y coordinates in the strain maps are given in pixels. These values can be transformed into micrometers with the pixel size that is specified in each figure; for example, 200 pixels in Figure 4 correspond to $2 \mu\text{m}$. The boundaries of the primary carbides are marked in the strain maps. Hereby, the M_6C -carbides marked by a cross in the centre. The

unmarked areas denote MC-carbides. The strain maps in Figure 4a, b show that the deformation is not homogeneous. ^bFirst plasticity occurs around the carbides. At higher loading small areas in the matrix material form straight shear bands that are predominantly oriented 45° to the loading direction. It is remarkable that the deformation pattern, when plotted in relative strains, does barely change between 2% and 8% global strain. Typical relative strains in the shear bands reach values of the $\kappa_{xx} \approx 1.8$ at $\varepsilon_{\text{global}} \approx 2\%$ and $\kappa_{xx} \approx 2$ at $\varepsilon_{\text{global}} \approx 8\%$; the maximum values are $\kappa_{xx} \approx 2.8$ and $\kappa_{xx} \approx 2.8$, respectively. This means that the martensitic matrix of the Böhler S390 Microclean can be subjected to a local strain of $\varepsilon_{xxl} \approx 22\%$ without any visible damage in the microstructure. Of course this is valid only for monotonic loading in compression.

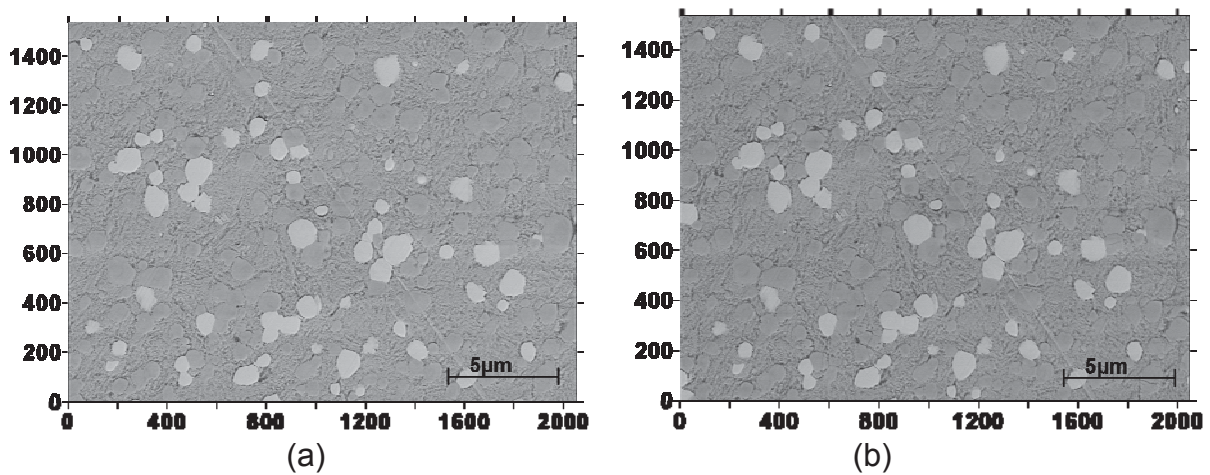


Figure 3: SEM micrographs of the PM-tool steel grade S390 Microclean at global strains in loading direction of (a) $\varepsilon_{\text{global}} \approx 2\%$, (b) $\varepsilon_{\text{global}} \approx 8\%$.

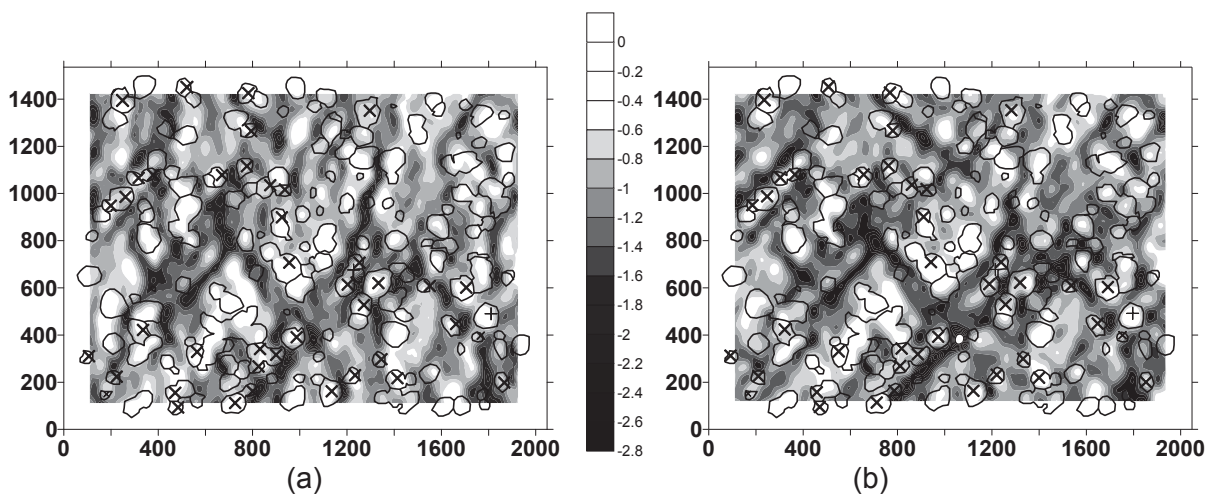


Figure 4: Local deformation behaviour of the PM-tool steel grade S390 Microclean. The loading direction is parallel to the horizontal axis. Plotted are the relative strains in loading direction κ_{xx} . (a) $\varepsilon_{\text{global}} \approx 2\%$, (b) $\varepsilon_{\text{global}} \approx 8\%$. Pixel size = 0.01 μm

^b Normally coloured strain maps are generated that exhibit much more details in higher resolution than the maps in black and white presented in this paper.

4. Deformation behaviour under cyclic loading

4.1. Experimental

Since cutting, blanking or stamping tools are cyclically loaded in service, and since the loading of the tools varies specially from the edge region to the interior, a testing procedure shall be developed that resembles better the actual loading conditions in such tools. This procedure shall be applicable especially to investigate the appearance of cracks near the tool edge. The deformation behaviour shall be studied not only at the free surface of the specimen, but also in the interior. Therefore, a special split-specimen experiment was developed, similar to the procedure applied in [13]. Figure 5 shows the test set-up with the specimens. The specimens have a thickness of 5 mm, a width of 10 mm, and a length of 15 mm. On the top of the pair of specimens a cylinder made of hard metal is positioned. One of the specimens is cut in the middle along the x-plane. The second specimen is not cut because its function is only to stabilise the hard metal cylinder. The cut front side was ground and mechanically polished with different diamond suspensions. After the specimen preparation SEM images are taken of the unloaded edge region, see the marked area in Figure 5a, b. Subsequently the specimens are mounted in the loading device. After four loading cycles, the specimen is demounted to take deformation micrographs in the SEM. If desired, the specimen can be demounted for additional cycles. Table 3 shows the parameters of the cyclic loading test. The analysis of the deformation micrographs yields again maps of the strains in the loading direction, ϵ_{xx} , the transverse strains, ϵ_{yy} , the shear strains, ϵ_{xy} , and the rotation r_{xy} .

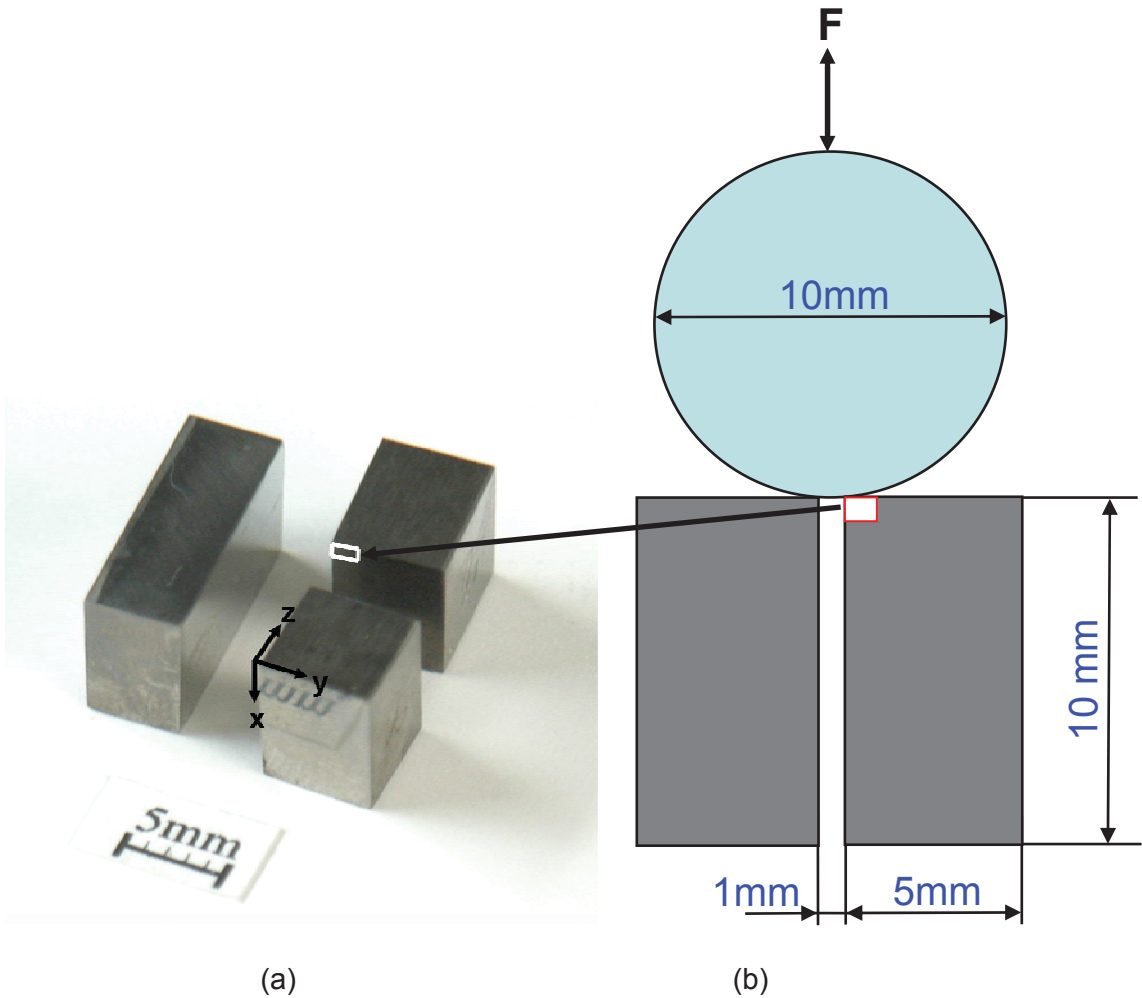


Figure 5: (a) Geometry of the split specimen (b) Test set up

Table 3: Parameters of the cyclic load test

| Fmax[N] | Fmin[N] | Frequency[Hz] | Alternation of load |
|---------|---------|---------------|---------------------|
| -1000 | -31000 | 10 | 4 |

4.2. Results and Discussion

In the following, the results of a first preliminary test are presented. The results are summarised in Figure 6 and Figure 7. Figure 6 shows the microstructure of the investigated area after four load cycles. The dotted lines show the geometry of the specimen after the loading. A scratch is visible in Figure 6 in the microstructure which probably was formed during mounting of the split specimens. Figure 7 presents the maps of the strain in loading direction ϵ_{xx} . The x-y coordinates in the strain maps are given in pixels; 100 pixels correspond to 10 μm . In the analysed area the local strains in loading direction vary between $\epsilon_{xx} \approx 0.28\%$ and $\epsilon_{xx} \approx 3.2\%$. The maximum strains in loading direction, ϵ_{xx} , appear near the upper edge, at a distance 30 and 70 μm from the corner point. The local strains in the loading direction show in the middle of the deformed zone a broad highly deformed zone that seems to originate from the boundary of the intended region at the upper surface. The maximum strains in this zone reach $\epsilon_{xx} \approx 3\%$. A second, small deformation band seems to be caused by the scratch. The strain map does not reach to the upper left corner of the analysed area. A probable reason is that the deformation is so high that the matching procedure does not work.

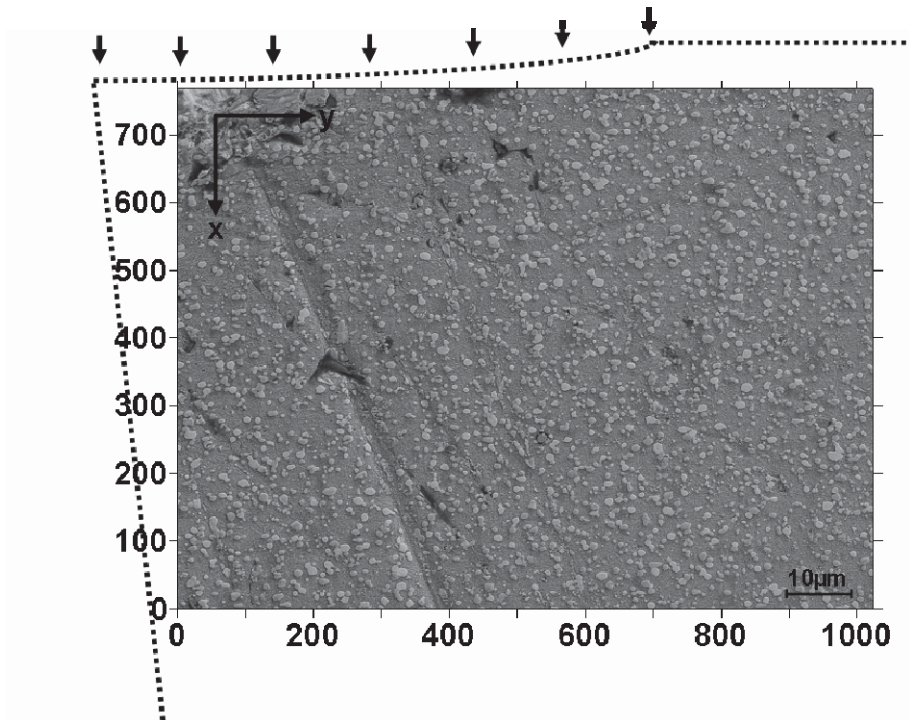


Figure 6: SEM micrograph of the deformed specimen after 4 load cycles

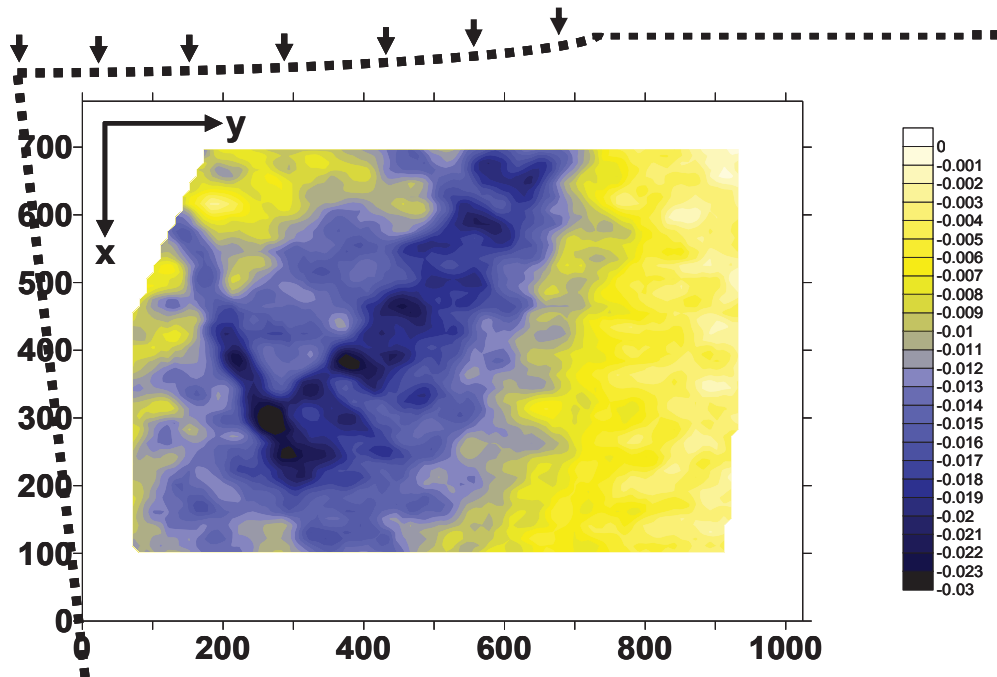


Figure 7: Local deformation behaviour of the PM-tool steel after 4 load cycles; local strains in loading direction ε_{xx} . Pixel-size=0.1 μ m.

5. Conclusions

Two testing procedures were developed: (1) an in-situ compression test for studying the behaviour under monotonic, macroscopically homogeneous loading; (2) a newly developed testing technique with an inhomogeneous loaded split specimen. This technique allows us to investigate the local deformation behaviour under cyclic loading from the interior to the tool edge where local plastic deformation may lead to the initiation and propagation of cracks. The quantitative analyses of the first experiments yield promising results. It is possible to investigate the local deformation behaviour of high strength tool steels with the digital image analysis. Furthermore, it is possible to investigate the plastic deformation near a cutting edge of high strength tool steels for a cyclic load experiment with the digital image analysis and to investigate the local deformation behaviour not only at the free surface of the specimen, but also in the interior.

Acknowledgments

Financial support by the Österreichische Forschungsförderungsgesellschaft mbH, the Province of Styria, the Steirische Wirtschaftsförderungsgesellschaft mbH and the Municipality of Leoben within research activities of the Materials Center Leoben under the frame of the Austrian Kplus Competence Center Programme is gratefully acknowledged.

References

- [1] Advanced High Strength Steels (AHSS) Application Guideline Version 3, International Iron Steel Institute, September 2006, online at www.worldautosteel.org
- [2] A.H. Fritz, G. Schulze (Hrsg.): Fertigungstechnik, 5.Aufl., Springer Verlag, Berlin Heidelberg, 2001, 235
- [3] H. Bhadeshia, R. Honeycomb: Steels, 3.Aufl. Elsevier Verlag, Amsterdam, 2006, 344
- [4] I. Maili, R. Rabitsch, W. Liebfahrt, H. Makovec, E. Putzgruber: Proceeding of the 6th international Tooling Conference, Vol. 1, Karlstad University 2002, Sweden, 377
- [5] B.Griffith: Manufacturing Surface Technology-Surface Integrity and Functional Performance, Penton Press, London, 2001
- [6] J. Hua, D. Umbrello, R.Shivpuri: Investigation of cutting conditions and cutting edge preparations for enhanced compressive subsurface residual stress in the hard turning of bearing steel, Journal of Materials Processing Technology 171, 2006, 180-187
- [7] Internal investigations of the Material Centre Leoben
- [8] A. Tatschl, O. Kolednik: A new tool for the experimental characterization of micro – plasticity, Mater Sci Eng 2003; A339:265–280
- [9] K.Unterweger, O.Kolednik: The local deformation behaviour of MMCs - an experimental study, Z.Metallkunde, 2005, 96:1063-8
- [10] O.Kolednik, K.Unterweger: The ductility of metal matrix composites – Relation to local deformation behavior and damage evolution, Engineering Fracture Mechanics, 2007, doi:10.1016/j.engfracmech.2007.08.011
- [11] P. Gruber: Lokale Verformungsanalysen von hochfesten PM-Werkzeugstählen, Diploma thesis, University of Leoben, 2006.
- [12] D.L. Davidson: The Observation and Measurement of Displacements and Strain by stereo imaging, Scanning Electron Microscopy 1979; 11:79-86.
- [13] G.Trattnig, T.Antretter, R.Pippan: Fracture of austenitic steel subject to a wide range of stress triaxiality ratios and crack deformation modes, Engineering Fracture Mechanics, 2007, doi:10.1016/j.engfracmech.2007.03.021